



Universiteit
Leiden
The Netherlands

Investigations of radiation pressure : optical side-band cooling of a trampoline resonator and the effect of superconductivity on the Casimir force

Eerkens, H.J.

Citation

Eerkens, H. J. (2017, December 21). *Investigations of radiation pressure : optical side-band cooling of a trampoline resonator and the effect of superconductivity on the Casimir force*. Retrieved from <https://hdl.handle.net/1887/59506>

Version: Not Applicable (or Unknown)

License: [Licence agreement concerning inclusion of doctoral thesis in the Institutional Repository of the University of Leiden](#)

Downloaded from: <https://hdl.handle.net/1887/59506>

Note: To cite this publication please use the final published version (if applicable).

Cover Page



Universiteit Leiden



The following handle holds various files of this Leiden University dissertation:

<http://hdl.handle.net/1887/59506>

Author: Eerkens, H.J.

Title: Investigations of radiation pressure : optical side-band cooling of a trampoline resonator and the effect of superconductivity on the Casimir force

Issue Date: 2017-12-21

Dependence of the Casimir Force on the Dielectric Permittivity of NbTiN

The magnitude of the Casimir force is determined by circumstances like the geometry of the system and the closest distance between the surfaces. Another important factor is the reflectivity of the surfaces. The reflectivity of the material can be determined via optical reflection measurements, and can be used to calculate the Casimir force via the method described in chapter 5. We have followed these steps to compute the force between a gold sphere and a superconducting plate. These calculations show very good agreement with Casimir force measurements obtained at room temperature.

The exact calculation of the Casimir force between real materials requires full knowledge of the complex dielectric permittivity of the materials [97, 98]. At high frequencies, we can rely on the measured optical spectra, but these are available only in a certain frequency range. At low frequencies, it remains uncertain whether to include Ohmic dissipation in the calculation of the Casimir force or not. Since dissipation is not present in superconductors, it has been proposed [49, 55] to measure the Casimir force between superconducting materials. Comparison of the Casimir force below and above the critical temperature may give insight into the low frequency contribution of the dielectric permittivity.

Measurements of the Casimir force gradient between a gold coated sphere with radius $R = 100 \mu\text{m}$ and a 150 nm thick gold layer on a sapphire substrate were shown in chapter 7. In that chapter we described our measurement method in detail, we will therefore not elaborate on that in this chapter. Here we will show the results obtained by exchanging the gold coated sapphire plate by a SiO_2 plate coated with a 200 nm thick layer of niobium titanium nitride (NbTiN), which is a superconductor below its critical temperature of 13.6 K. The Casimir force is measured as a function of distance at two different temperatures, below and above the critical temperature, and as a function of temperature at a distance of 83 nm. We detect no large influence of the superconducting transition on the strength of the Casimir force.

8.1 Casimir force computed from the measured optical spectrum of NbTiN

In chapter 7 we demonstrate the accurate calibration of our system by comparing measurements with calculations of the Casimir force between two gold surfaces. To compute the Casimir force, we used optical reflection measurements of gold [112]. Extrapolation to frequencies where these data are incomplete can be done based on the Drude or on the plasma model, using the plasma and relaxation frequencies that can be obtained from a fit to the optical reflection data. We are interested in the Casimir force between gold and NbTiN, but a comparison with computations could not directly be obtained due to the lack of optical reflection data on NbTiN in literature [167]. We therefore sent our NbTiN sample to Erik van Heumen from the optical spectroscopy lab at the University of Amsterdam [168], who measured the optical spectrum between 1 cm^{-1} and $60\,000 \text{ cm}^{-1}$ (between $1.89 \times 10^{11} \text{ rad/s}$ and $1.13 \times 10^{16} \text{ rad/s}$). The dielectric permittivity of our sample was calculated via a fit of the reflection data and its real and imaginary part are shown in Figure 8.1. The optical spectrum was measured at room temperature and at lower temperatures, since the spectrometer is combined with a cryostat. Figure 8.1 also shows the permittivity at 16 K, the base temperature of that cryostat.

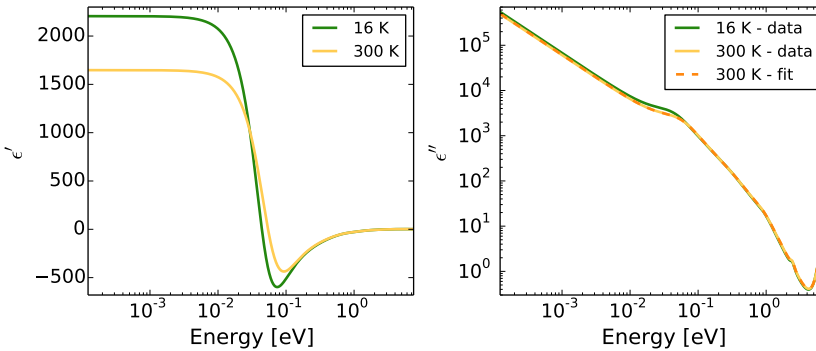


Figure 8.1: Dielectric permittivity of NbTiN as a function of frequency, measured at the optical spectroscopy lab at the University of Amsterdam, both at room temperature and at 16 K: (a) Real part; (b) Imaginary part, a fit to the room temperature spectrum based on the Drude model combined with Lorentz oscillators is also shown.

Extra resonances resulting from the restoring force that binds the core electrons to the nuclei [116] are visible in the spectra. A fit to the imaginary part of the spectrum, shown in Figure 8.1(b) for the room temperature data, based on the imaginary part of the Drude-Lorentz model,

$$\epsilon''_{\text{DL}}(\omega) = \frac{\Omega_p^2 \gamma}{\omega(\omega^2 + \gamma^2)} + \sum_j^K \frac{f_j \beta_j \omega}{\beta_j^2 \omega^2 + (\omega_{0j}^2 - \omega^2)^2}, \quad (8.1)$$

yielded $K = 4$ resonances with resonance frequencies ω_{0j} at 0.059 eV, 0.88 eV, 2.4 eV and 6.2 eV respectively. Their oscillator strengths f_j and damping rates β_j were also found, as well as values for the plasma frequency $\Omega_p = 43\,000\text{ cm}^{-1} \approx 5.33\text{ eV}$ and relaxation rate $\gamma = 3750\text{ cm}^{-1} \approx 0.465\text{ eV}$ at room temperature and $\gamma = 3350\text{ cm}^{-1} \approx 0.415\text{ eV}$ at 16 K. Based on these values, the dielectric permittivity at imaginary frequencies is given by the Drude-Lorentz model

$$\varepsilon_{\text{DL}}(i\xi) = 1 + \frac{\Omega_p^2}{\xi(\xi + \gamma)} + \sum_j \frac{f_j}{\omega_{0j}^2 + \xi^2 + \beta_j \xi}, \quad (8.2)$$

or by the generalized plasma model

$$\varepsilon_{\text{gp}}(i\xi) = 1 + \frac{\Omega_p^2}{\xi^2} + \sum_j \frac{f_j}{\omega_{0j}^2 + \xi^2 + \beta_j \xi}. \quad (8.3)$$

For comparison, we also integrate the imaginary part of the dielectric permittivity via the Kramers-Kronig relations (see Eq. 5.12), after we extrapolate the data to lower and higher frequencies according to the Drude model. This should lead to the same dielectric permittivity at imaginary frequencies as described by the Drude-Lorentz model.

From these dielectric permittivities, the reflectivity of the surfaces is then determined via the Fresnel equations. The Casimir pressure between gold and NbTiN is found by putting in the appropriate reflectivities in Eq. 5.11. Finally, to compare the calculated parallel plate pressure with our measurements of the Casimir force gradient in the sphere-plate geometry, we use the proximity force approximation [137, 138].

8.1.1 Comparison to room temperature measurements

For a detailed description of the set-up and measurement scheme, we refer to chapters 6 and 7. The room temperature data shown here were obtained with the following settings. Compensation of the contact potential difference V_0 was done via the FM side-bands at ω_1 . We first performed a measurement run based on an educated guess of the system parameter μ . From the fit to the frequency deviation $\Delta f_{2\omega_1}$ as a function of separation we determined a value $\mu = 1.9 \times 10^{-12}\text{ Hz m}^2\text{ V}^{-2}$, close to the calculated value of $3.6 \times 10^{-12}\text{ Hz m}^2\text{ V}^{-2}$ based on values of $f_0 = 2.3\text{ kHz}$, $R = 100\text{ }\mu\text{m}$ and $k \approx 1\text{ N/m}$. During the measurements shown here the distance was set by a feedback loop that adjusted the piezo-electric transducer under the plate until the set-point at the $2\omega_1$ FM side-bands was reached, via the relation

$$d = \sqrt{\frac{\mu V_{\text{AC}}^2}{2\Delta f_{2\omega_1}}}. \quad (8.4)$$

The set-point was $\Delta f_{2\omega_1} = 0.54\text{ Hz}$, corresponding to a force gradient modulation with an amplitude of $4.7 \times 10^{-4}\text{ N/m}$ at the frequency $2\omega_1$.

The room temperature measurements shown here were obtained in the same cryostat as the low temperature measurements shown later in this chapter. The

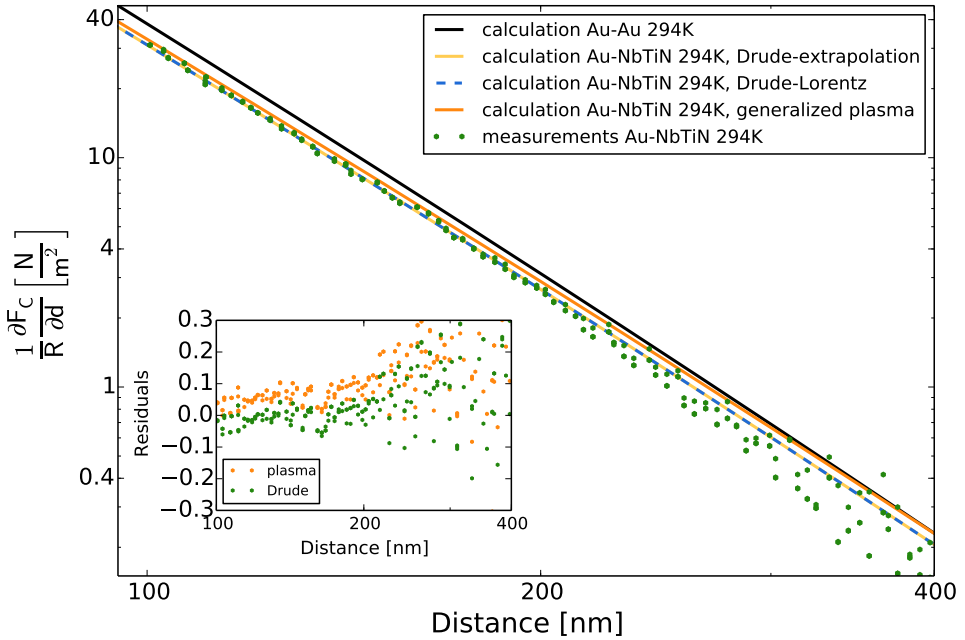


Figure 8.2: Measured Casimir force gradient, normalized to the sphere radius, between a gold coated sphere and a NbTiN thin film at room temperature (green dots). The lines indicate calculations of the Casimir force gradient at room temperature, between two gold surfaces (black line) and between gold and niobium titanium nitride. Three methods, discussed above, were used to determine the dielectric permittivity for NbTiN at imaginary frequencies: the Drude model based on extrapolation of the data (yellow line), the Drude-Lorentz model (blue dashed line) and the generalized plasma model (orange line). The good overlap between the calculations and measurements in general shows our control of the measurement as well as our ability to base calculations on actual optical reflection data. Compared to the calculations between two gold surfaces there is a decrease of about twenty percent in the force gradient between gold and NbTiN. The inset shows the difference between the calculations and data for the Drude-Lorentz and generalized plasma models, normalized to the model values.

background pressure in the cryostat was 6.2×10^{-2} mbar. A four stage mass-spring system, in fact the mechanical equivalent of an electrical wave filter [94, 169], was used to isolate the set-up from vibrational noise. To check that the data are not accidentally influenced by the surroundings, we have repeated our measurements in different circumstances. The same results were obtained in a different cryostat, with a different gold coated sphere, a different NbTiN plate and with the distance lock and electrostatic compensation done via the quasi-static signals.

The green dots in Figure 8.2 show the Casimir force gradient normalized to the sphere radius measured at room temperature. The lines show calculations of the normalized Casimir force gradient at room temperature. The dielectric permittivity of NbTiN at imaginary frequencies is determined via the three methods described above: via extrapolation of the optical data using the Drude model (yellow line), via the Drude-Lorentz model accounting for resonances in the material (blue dashed line) and via the generalized plasma model (orange line). The first two methods lead to the same Casimir force gradient, as can be expected. Using the generalized plasma model results in a stronger force gradient, at small separation the deviation is about five percent. This is significantly more than between two gold surfaces (compare Figure 5.4). As already explained in chapter 5, due to the higher resistance of NbTiN compared to gold, the two models diverge already at a higher frequency. The two models lead to different contributions to the Casimir force not only at the zero Matsubara frequency, but at higher order Matsubara frequencies as well. At room temperature, at the first eight or nine Matsubara frequencies the two models predict different contributions, while about a hundred frequencies contribute in total. Measuring the Casimir force between high resistive materials therefore seems a prudent way to distinguish between the Drude and plasma models [170].

If we compare our data with our calculations between gold and NbTiN, we notice the good general overlap. Note that the lines are not fits and that the measurements and calculations were obtained in two completely independent ways. The overlap shows both our control and good calibration of the measurements and our ability to base Casimir force calculations on measured optical spectra. Taking a closer look at the overlap between the data and the computations based on the plasma and Drude models, we observe that the data seem to coincide better with the Drude model than with the plasma model. This is illustrated by the inset in Figure 8.2, which shows the difference between the data and Drude-Lorentz model (green dots) and between the data and generalized plasma model (orange dots), normalized to the values calculated by the models. This shows that for distances up to 200 nm, the data deviate $6.2 \pm 2.8\%$ from the plasma model and $0.4 \pm 2.7\%$ from the Drude model. This is just one measurement run, but other data runs show the same trend. Note that in general, the presence of an extra (electrostatic) force that is not calibrated in the experiments may lead to an overestimation of the Casimir force [165], an underestimation of the force is less likely [107]. More extensive data analysis, combined with more measurements, is required to draw a more definitive conclusion.

When we compare our data and calculations with calculations between two gold surfaces at room temperature (black line in Figure 8.2, equal to the line in Figure 7.8), we notice that the force between gold and NbTiN is twenty percent weaker than between two gold surfaces. This is a direct result of the smaller dielectric permittivity

of NbTiN. A decrease of twenty percent is substantial, different metallic surfaces produce nearly the same Casimir force [98]. For comparison, the Casimir force between gold and indium tin oxide (ITO), which is transparent in a large frequency range, reduces the force by about 40-50% [144].

Since the Drude model accounts correctly for Ohmic resistivity, it would seem more prudent to base calculations of the Casimir force on this model. However, certain measurements coincide better with the plasma model description that does not take Ohmic dissipation into account [11, 52, 107, 124]. These measurements were obtained at short distances, where the difference between the two models is relatively small. Measurements at a larger separation on the other hand have indicated a better accordance with the Drude model [50]. To our knowledge, the measurements shown in this chapter are the first that demonstrate a better overlap with the Drude model description at small separation.

8.2 Low temperature measurements

The measurements were repeated at 13.9 K, just above the critical temperature, such that the NbTiN is not yet superconducting. The orange squares in Figure 8.3 show these results. These data were obtained in the same circumstances as the room temperature measurements, except that the electrostatic compensation and distance lock were set on the quasi-static signals (set-point $50 \mu\text{V}_{\text{rms}}$, or 0.7 nN amplitude). Although the FM side-bands were not stable enough to be used for feedback, they were still recorded. A value for the system parameter could be determined as $\mu = 2.4 \times 10^{-12} \text{ Hz m}^2 \text{ V}^{-2}$. The small change compared to the room temperature value can be explained by a change in spring constant. This is also apparent in the resonance frequency, which shifts 60 Hz upwards from room temperature to low temperatures.

At low temperature, the Casimir force gradient has increased significantly compared to room temperature. We can even deduce an increase of the order of twenty percent. This cannot be an effect of the thermal Casimir force [50, 97], which is only a fraction of the zero-point contribution even at room temperature. Another explanation would be the change in the optical reflectivity of the surfaces. The reflectivity of gold is slightly temperature dependent [171, 172], but this influence is negligible [120]. The low temperature dielectric permittivity of NbTiN is measured and shown in Figure 8.1. Based on this optical spectrum we calculate via the Drude-Lorentz model the expected Casimir force at 16 K, equal to the temperature at which the optical spectrum of NbTiN was obtained. Figure 8.3 shows the result, denoted by the blue line. If we overlap the calculated Casimir force gradient at 16 K with the calculations at room temperature (the blue dashed line in Figure 8.3), we see that the force gradient differs only slightly between the two temperatures. It is clear that the change in reflectivity cannot account for the change in Casimir force gradient. Also if we base our calculations on the generalized plasma model, as indicated by the yellow line in Figure 8.3, the increased Casimir force gradient cannot be explained.

The black line shows the Casimir force gradient between two gold surfaces at 16 K, from the overlap between this line and the data, it would almost seem that the

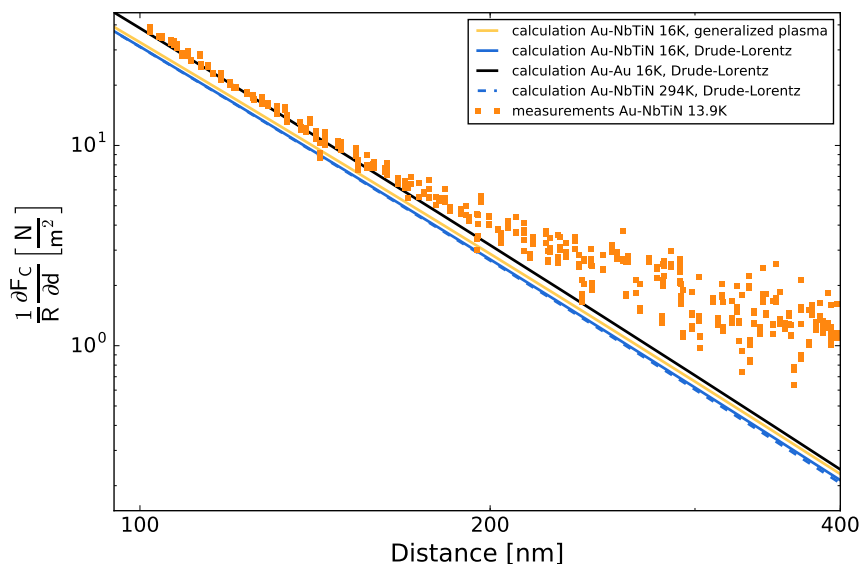


Figure 8.3: Casimir force gradient, normalized to the sphere radius, between a gold coated sphere and a NbTiN thin film measured at 13.9 K (orange squares). The solid lines indicate calculations of the Casimir force between gold-gold and gold-niobium titanium nitride at 16 K, based on the Drude-Lorentz model (blue line) as well as on the generalized plasma model (yellow line). The blue dashed line shows the calculated Casimir force gradient between gold and NbTiN at room temperature (equal to the yellow line in Figure 8.2). It is remarkable that the data overlap best with the calculations between two gold surfaces (black line), since we would expect an overlap with the calculated force gradient between gold and NbTiN (blue or yellow line).

NbTiN surface appears metallic for the Casimir force. To confirm these measurements, we repeated these measurements at temperatures between 9.3 K and 22 K, and at different cool-down runs. All these low temperature data overlap within our measurement error. This effect of increased Casimir force gradient should therefore begin at higher temperatures. It would be interesting to repeat our experiments in the temperature regime between 22 K and room temperature. If we take a look at low temperature measurements reported in literature, comparison between measurements at room temperature and at 77 K show no discrepancy [54]. Measurements at 4 K did report a ten percent difference, but ascribed it to an outdated system calibration [51].

We have no explanation for the increase in the detected Casimir force gradient at low temperatures. It may still have a technical cause. However, our room temperature calibration measurements between two gold surfaces (see Figure 7.8), as well as the good overlap between theory and our room temperature gold-NbTiN measurements (Figure 8.2) show that our measurement scheme is well capable of calibrating the sphere-plate distance and the sensitivity of our force sensor. For a conclusive

indication of the validity of our calibration scheme at low temperatures we would need to precede our low temperature Casimir force measurements between a gold sphere and NbTiN plate with calibration measurements between the sphere and a gold plate, during the same cool-down and under the same circumstances.

We are ultimately interested in the effect of the superconducting transition to the Casimir force. Since this results in a relative change, an absolute calibration of our set-up does not seem to be a strict requirement. The room temperature measurements convince us that we are indeed capable of measuring the Casimir force. However, we need to be cautious to ascribe any change across the superconducting transition to a change in the Casimir force.

8.2.1 The effect of superconductivity

In chapter 5 we discussed that measuring the Casimir force between superconductors may give insight in the uncertain contribution of the dielectric permittivity at low frequencies. The dielectric permittivity of a superconductor differs from the normal state in two ways. First is that static magnetic fields are expelled. Another change is the opening of the superconducting gap at high frequencies, which leads to a zero resistivity of the material. Both effects may have measurable impact on the Casimir force. These effects become greater when the temperature approaches 0 K. It is therefore optimal to measure the force over a large temperature range below the critical temperature, but unfortunately the base temperature of our cryostat was limited to 9.3 K. However, our measurements still allow us to impose an upper limit on the effect of superconductivity on the Casimir force.

In Figure 8.4 we show the normalized Casimir force gradient as a function of distance measured just below (9.3 K) and just above (13.9 K) the critical temperature of our NbTiN plate (13.6 K). The data were obtained during the same cool-down under equal circumstances. For both measurements, the electrostatic compensation of the contact potential difference V_0 was done via the quasi-static signal S_{ω_1} . The distance lock was set on the quasi-static signal $S_{2\omega_1}$ with a set-point of $50 \mu V_{\text{rms}}$ corresponding to a force modulation with an amplitude of 0.6 nN at the frequency $2\omega_1$, based on a spring constant of 1 N/m and interferometric read-out sensitivity of 125 kV/m. The force sensitivity, deduced from the fit to $S_{2\omega_1}$ as a function of separation, had a value of $\kappa = 2.56 \times 10^{-10} \text{ m V}^{-1}$ at 9.3 K and $\kappa = 2.48 \times 10^{-10} \text{ m V}^{-1}$ at 13.9 K. The difference can be explained by a small deflection of the cantilever that is caused by the change in temperature, which in turn causes a change in the interferometric read-out sensitivity γ .

The calculation of the Casimir force between two gold surfaces at 16 K is also depicted in Figure 8.4 as a guide to the eye. The choice for this calculation is motivated by the low temperature results shown above. At distances larger than 200 nm the data points start to deviate towards our measurement precision of 1.5 N/m^2 .

The Casimir force measurements below the critical temperature overlap with the measurements above the critical temperature, at least within our measurement accuracy. We can therefore conclude that there is no significant influence of the superconducting state. There is definitely no new, unexpected effect that has a significantly greater influence on the Casimir force than what we predicted based on the

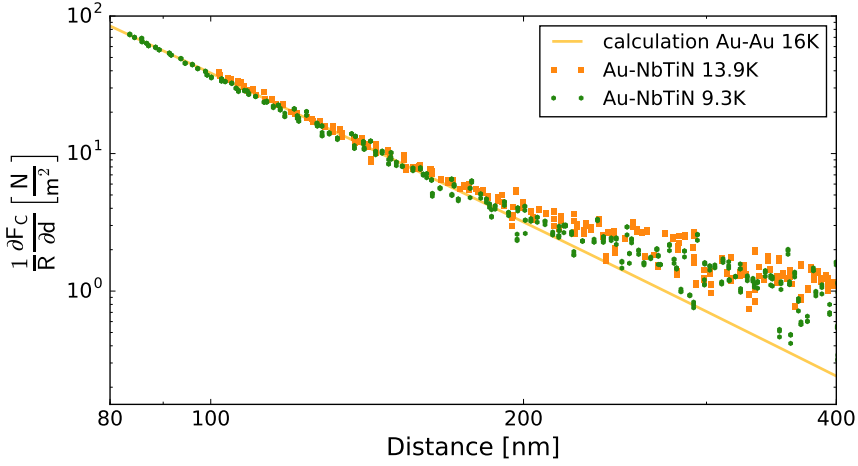


Figure 8.4: Casimir force gradient, normalized to the sphere radius, between a gold coated sphere and a NbTiN thin film as a function of distance. The film was in a superconducting state at 9.3 K (green dots) and in a normal state at 13.9 K (orange spheres). Within our measurement accuracy we can set an upper limit of about seven percent on the effect of superconductivity to the Casimir force.

possible change in reflectivity of the superconductor. To make this statement more quantitative, we take a closer look at the force at a distance of 120 nm. Values for the normalized force gradient are indicated in Table 8.1. From these values we can deduce that the effect of the superconducting state is less than seven percent.

Temperature	Normalized force gradient
9.3 K	$20.9 \pm 1.5 \text{ N/m}^2$
13.9 K	$21.8 \pm 1.2 \text{ N/m}^2$

Table 8.1: Casimir force gradient, normalized to the sphere radius, between a gold coated sphere and a NbTiN plate at a distance of 120 nm at two different temperatures, just below and just above the critical temperature of the plate.

Since the precision of 1.5 N/m^2 is constant over distance, we can improve on this limit by measuring at a smaller separation. Our measurement method allows us to keep the distance fixed even when circumstances like the temperature change. It is therefore possible to do a temperature sweep of the Casimir force gradient. Since we monitor the plate conductance simultaneously, we can directly indicate the superconducting transition in our measurements. These measurements are shown in Figure 8.5. Since the cantilever may deflect as the temperature changes, the interferometric read-out sensitivity γ can change, which will influence the force sensitivity κ . It is therefore not possible to set the distance lock on the QS signal $S_{2\omega_1}$. We set it instead on the FM side-band $\Delta f_{2\omega_1}$, with a set-point of 1 Hz ($8.7 \times 10^{-4} \text{ N/m}$). The sys-

tem parameter was determined from a previous measurement of the Casimir force gradient as a function of distance and was found to be $\mu = 2.22 \times 10^{-12} \text{ Hz m}^2 \text{ V}^{-2}$. We set the AC bias voltage between the sphere and the plate such that the PI feedback loop will set the distance to 83 nm. Note that a deviation in the distance of about 1.5% will result in a variation in the measured force gradient of about 6%. With resistance heaters in the cryostat we sweep the temperature. During the run the temperature was increased from 10.2 K to 14.5 K before the heaters were switched off again, lowering the temperature to 10.4 K. The output of the resistance bridge that monitors the plate resistance (described in chapter 7) is shown in Figure 8.5(a). The green dots show the data during the temperature increase, the data obtained during the downward sweep are depicted in orange. The superconducting transition occurred at a value of 12.5 K on the plate thermometer. This is lower than the expected critical temperature of 13.6 K. The difference can be caused by a larger temperature gradient between the thermometer and plate due to a higher heating rate than we used to determine the critical temperature in chapter 7. Since we determine the superconducting transition based on the plate's resistance and not on the temperature, this is not an issue.

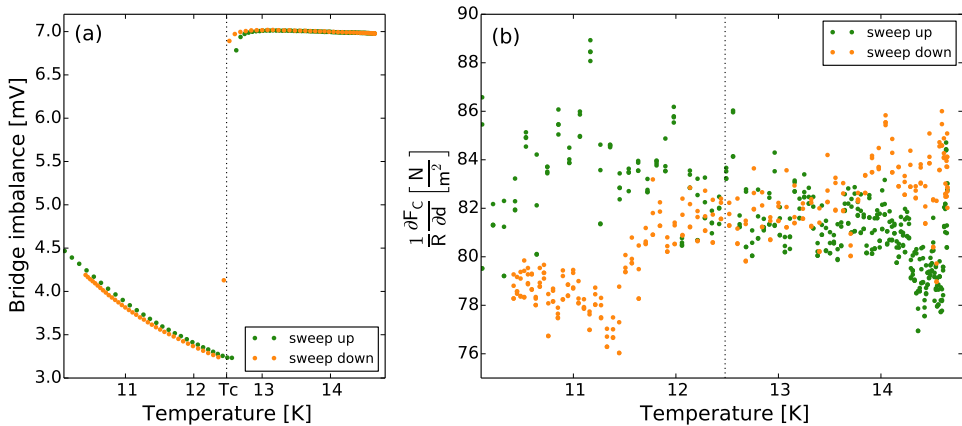


Figure 8.5: Temperature dependency of the Casimir force: (a) The simultaneous resistance measurement of the plate detects the superconducting transition at a temperature of 12.5 K; (b) Casimir force gradient at a distance of 83 nm as a function of temperature, the superconducting transition is indicated by the dotted vertical line.

The normalized Casimir force gradient as a function of temperature is shown in Figure 8.5(b). The sweep up is indicated in green, the downward sweep in orange. The superconducting transition is indicated by the dotted line. Above the critical temperature the Casimir force gradient, normalized to the sphere radius, is equal to $81 \pm 2.1 \text{ N/m}^2$. The expected change with temperature, based on the theory developed in chapter 5, depends on which model is used to extrapolate the dielectric permittivity. If we use the (generalized) plasma model, we expect no temperature dependence. The Drude-Lorentz model predicts an increase of the force as the tem-

perature is lowered, of about 5% between the critical temperature and $T \ll T_c$. This number is an overestimation since we use the two-fluid model for our prediction, which does not account for impurity scattering [134]. Since we only measure at temperatures around T_c , and not at $T \ll T_c$, the force should not have increased maximally yet. But we can still expect a change of 3.4% between our data at the lowest temperature and above the critical temperature when the low frequency permittivity of the normal state of NbTiN is described by the Drude model instead of the plasma model.

If we look at the data in Figure 8.5(b), we see no such increase in the force below the critical temperature. It seems that two branches appear below 12 K, but a similar deviation is visible above 14 K. We are not sure what causes this effect, but we do not exclude that it is caused by small fluctuations in the distance. The deviations in the measured force gradient of about 5 N/m^2 can be explained by an imprecision in the distance of about 1.3 nm at 83 nm. We need to repeat this measurement after minimizing the effect of noise in our distance lock in order to give a more conclusive answer to the effect of the superconducting transition on the Casimir force.

If we compare our accuracy of 2.1 N/m^2 to the average force gradient that we measured, we can set an upper limit of 2.6% of the influence of the superconducting state to the Casimir force. This is in the same order of magnitude as the maximally expected effect obtained from calculations based on the Drude-Lorentz model. Recall that the plasma model predicts no measurable changes. Although, at first glance our upper limit seems to be smaller than the effect predicted by the Drude model, we must be careful to draw conclusions. The estimation is likely to be too large, as was mentioned above. Furthermore, we cannot guarantee that the distance is fixed within 0.2 nm at 83 nm, such that changes in the force of the order of a percent cannot be ascribed to or concealed by changes in the distance.

There is another effect that may lessen the effect of the superconducting state. The Casimir force is mostly determined by the surface modes of the material [36, 173], as it depends on the penetration depth of the electromagnetic fields. Very simply put, the bulk properties are screened by the surface. This penetration depth varies with frequency and depends on the plasma and relaxation frequencies, we estimate it to be of order 100 nm. Superconductors, on the other hand, are characterized by their coherence length ξ_0 . This length can be interpreted as the distance from the surface over which the density of superconducting Cooper pairs recovers to the bulk value assumed in our calculations [174]. This means that at the surface, up to the coherence length, the material cannot be considered as a full superconductor. The effect of the superconducting state on the Casimir force can only be measured if the coherence length is significantly shorter than the penetration depth. And even then, the effect is less than what we have calculated based on bulk values of the superconducting electron density only. We can only make an estimate of the coherence length of our NbTiN sample based on literature [167], which is $\xi_0 = 170 \text{ nm}$. But the coherence length depends on temperature, such that it diverges at the critical temperature and becomes significantly smaller near 0 K. Correctly taking the surface effects into account will therefore lead to a smaller effect of superconductivity, but approaches our bulk value calculations near $T \ll T_c$. We therefore need to repeat our measurements at significantly lower temperatures.

However, it is already a significant result to set an upper limit of 2.6% on the effect of superconductivity, significantly larger than the effect predicted by the plasma model, but of the same order as the effect predicted by the Drude-Lorentz model. This means that only small improvements are needed to be able to distinguish the effect of the superconducting state.

8.3 Conclusion

The Casimir force depends on the reflectivity of the interacting surfaces. When the dielectric permittivity of a material is known, the Casimir force can be calculated. We have shown these calculations based on optical reflection measurements of NbTiN. The computed Casimir force gradient is then compared to measurements between a gold coated microsphere and a NbTiN thin film. At room temperature, the overlap with the calculations is striking. Due to the higher resistivity of NbTiN compared to gold, the Drude-Lorentz and generalized plasma models coincide at a higher frequency, such that even at room temperature the two models predict different contributions at higher order Matsubara frequencies. The two models lead to a significant difference in the Casimir force gradient that is detectable even with moderate sensitivity at close distances. Our measurements show better agreement with the Drude-Lorentz description and seem to exclude the plasma description.

At low temperatures, the experiments showed a twenty percent increase in the measured Casimir force, which does not coincide with our calculations of the force at these temperatures. We could find no satisfying explanation for this effect. However, our real-time calibration scheme and the good overlap between theory and experiment at room temperature convince us that the measurements are not dominated by other forces or drifts in the system between the moment of calibration and the measurements. Measurements of the Casimir force between 22 K and room temperature will demonstrate when this effect occurs and whether the transition is gradual or sudden. Comparison to Casimir force measurements between two gold surfaces at low temperature will exclude any technical errors leading to this effect. The measurements seem to indicate that the NbTiN plate behaves metallic, although optical reflection measurements do not show this behaviour. This may indicate that Casimir force measurements can provide new information on the reflection and conductance properties of materials that are not visible with other experiments.

Measuring the Casimir force between superconductors is a good way to gain insight in the role of dissipation in the Casimir force [49, 55], since dissipation becomes absent in superconductors. Our experiments show no significant influence of the superconducting state and can set an upper limit of 2.6% on its effect. This is of the same order of magnitude as the expected effect of superconductivity on the Casimir force, if such an effect exists.